Proceedings of ASME Turbo Expo 2011
GT2011
June 6-10, 2011, Vancouver, British Columbia, Canada

GT2011-46293

DYNAMIC CHARACTERISTIC ANALYSIS OF A ROTOR-BEARING SYSTEM USING GLOBAL ASSUMED MODE METHOD WITH DIFFERENT POLYNOMIAL FUNCTION

T. N. Shiau *, Professor
J. R. Chang**, Associate Professor
C. H. Kang***, Assistant Professor
C. Y. Liao *, Graduate

* Department of Mechanical Engineering
National Chung Cheng University
621 Chiayi, Taiwan, R.O.C.

** Department of Mechanical Engineering
Air Force Institute of Technology
820 Kaoshung, Taiwan, R.O.C.

*** Department of Greenergy
National Tainan University
700 Tainan, Taiwan, R.O.C.

ABSTRACT

In this study, the dynamic analysis of a domestic high speed rotor bearing system in turbo machines by using global assumed mode with different polynomial is investigated. This system consists of rotating multi flexible shaft, rigid disks and stiffness bearing effects. The analysis includes the whirl speeds, critical speeds, and mode shapes. The Global Assumed Modes Method (GAMM) and Finite Element Method (FEM) are employed to model the rotor-bearing system, and the accuracy of the results is discussed. With the application of GAMM, similarity transformation of different types of polynomials and interval has been investigated. The results show that using different polynomial function in GAMM have similar results, and which are also be agreed with the FEM. The results also show that the number of polynomial can be increased as the interval of the assumed mode function is altered. Consequently, the convergence of higher order modes will be more accurate.

Keywords: rotor bearing system, global assumed modes method, finite element method, Chebyshev polynomial, Legendre polynomial

I. INTRODUCTION

Several numerical approximations have been developed to analyze the dynamic behavior of rotor bearing system. The Finite Element Method (FEM) was popular in the published literatures for the analysis of the rotor dynamics. Ruhl and Booker [1] applied the finite element technique to study the dynamics of rotor system, but their study only included the translational inertia and bending stiffness. Many other important effects such as the rotary inertia, shear deformation and gyroscopic moments were neglected. Nelson and McVaugh [2] improved Ruhl's model [1] with a Rayleigh beam finite element model. It was included the effects of rotary inertia, gyroscopic moments, viscously damped bearings and axial load for a flexible rotor system supported on elastic supports. Zorzi and Nelson [3] extended the work by incorporating the effects of both internal viscous and hysteretic damping in the same model. Nelson [4] also utilized Timoshenko beam theory for establishing the shape functions. Based on the shape functions, he derived the system matrices of governing equations. The governing equations can be quickly changed into a Rayleigh beam or Euler beam model if the shear parameter is zero. Özqüven and Özqkan [5] presented the combined effects of shear deformations and the internal damping in their finite element formulation. They analyzed the natural whirl speeds and unbalance response of multi-bearing rotors in their study. Many other works which utilized the finite element technique for rotor dynamic analysis can be found in [6, 7, 8 and 9]. Those works showed that using finite elements for the modeling of rotor-bearing systems sometime makes the formulation be complicated. The Generalized Polynomial Expansion Method (GPEM), which was proposed by Shiau and Hwang [10, 11 and 12], is employed in this paper. The method described the deformations of rotating shaft with a series of polynomials. This method can be applied to both linear and nonlinear rotor systems. Shiau also demonstrated the efficiency and accuracy by using the GPEM as compared with the FEM in their studies. Shiau et al. [13] used the Timoshenko beam model to devise the global assumed mode formulation. In their study, they called the GPEM as a different name: "Global Assumed Mode Method" (GAMM). The GAMM was used to analyze the dynamic behavior of a spinning Timoshenko beam which is subjected to a moving skew force with different general boundary conditions.

NOMENCLATURE

A	:	Cross section area of the shaft
(a_n, b_m)	:	Coefficients of polynomial
E	:	Modulus of elasticity
e		Eccentricity distribution of the shaft
e_i^d		Eccentricity of the i-th disk
$[G]$	:	Gyroscopic matrix

$[I]$	:	Unit matrix
I	:	Area moment of inertia of the shaft
I_D, I_P	:	Diametral and polar mass moment of inertia distribution of the shaft
I_{Di}^d, I_{Pi}^d	:	Diametral and polar mass moment of inertia distribution of the *i*-th disk
$[K]$, $[K_S]$	:	System stiffness and shaft stiffness matrices
$[K_{yy}],[K_{zz}]$	:	Direct stiffness matrix for linear supports
$[K_{yz}],[K_{zy}]$	:	Cross coupled stiffness matrix for linear supports
k_{yyj}^b, k_{zzj}^b	:	Direct stiffness coefficients of the *j*-th bearing
k_{yzj}^b, k_{zyj}^b	:	Cross coupled stiffness coefficients of the *j*-th bearing
l	:	Total length of the shaft
$[M_T],[M_R]$	:	Translational and rotational mass matrices
m_i^d	:	Mass of the *i*-th disk
N_d, N_b	:	Total number of disk and bearing
N_P	:	The number of terms of polynomial
P_n	:	Legendre polynomials
q	:	Generalized coordinates vector represents coefficient vector *a* and *b*
R_a, R_b	:	Vectors of generalized forces
$[S]$	:	Similarity transformation matrixes
T	:	Total kinetic energy
T_S, T_d, T_e	:	Kinetic energy contributed by flexible shaft, rigid disk and mass eccentricity
T_n	:	Chebyshev polynomials
U	:	Total potential energy
U_S, U_b	:	Potential energy components by flexible shaft and bearing
U_n^j	:	Strain energy stored in *j*-th bearing for the *n*-th natural whirl mode
(V, W)	:	Lateral deflection in (Y,Z) directions
(V_i^d, W_i^d)	:	Lateral deflection of the *i*
(V_j^b, W_j^b)	:	Lateral deflection of the *j*
X-Y-Z	:	Fixed reference frame
x-y-z	:	Rotating reference frame
x_i^d, x_j^b	:	Positions of the *i*-th disk and the *j*-th bearing
α_r	:	Real part of eigenvalues
(B,Γ)	:	Angle of rotation about (Y,Z) axes
λ	:	Whirl ratio $(\lambda = \Omega/\omega)$
ρ	:	Mass density per unit volume of the shaft
ϕ	:	Generalized polynomial vector
φ	:	Phase angle
ω, Ω	:	Whirl speed and rotating speed
ω_n^c	:	The n-th critical speed

Ⅱ. DYNAMIC ANALYSIS OF LINEAR ROTOR-BEARING SYSTEM

Figure 1 shows the configuration of simple rotor-bearing system, which usually consists of rotating flexible shaft, rigid disks and bearings. Two reference frames are utilized to describe the system motion. One is a fixed reference frame X-Y-Z, and the other is a rotating reference x-y-z. The rotating frame rotates about the X axis with a whirl speed of ω. Ω denotes the rotating speed of shaft about the X axis.

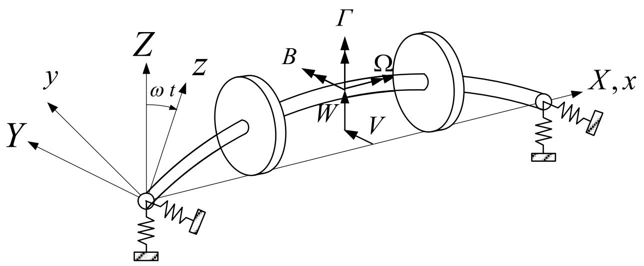

Figure 1 The configuration of simple rotor-bearing system.

The deflections of the cross section of shaft include two translations (V, W) and two rotations (B, Γ). By this assumption, the deflections as functions of positions along the rotating axis x and time t. Which are expressed as:

$$\begin{aligned} &V = V(x,t), \;\; W = W(x,t) \\ &B = B(x,t), \;\; \Gamma = \Gamma(x,t) \end{aligned} \tag{1}$$

The rotations (B, Γ) are related to the translations (V, W) as

$$B(x,t) = -\frac{\partial W(x,t)}{\partial x}, \;\; \Gamma(x,t) = \frac{\partial V(x,t)}{\partial x} \tag{2}$$

With the GAMM [10], the associated deflections can be expressed as

$$V(x,t) = \sum_{n=1}^{N_p} a_n(t) x^{n-1}, \;\; W(x,t) = \sum_{m=1}^{N_p} b_m(t) x^{m-1} \tag{3}$$

The Lagrangian approach is used to derive the equation of system motion. The kinetic energy T and the potential energy U of the rotating shaft are given by

$$\begin{aligned} &U = U_s + U_b \\ &T = T_s + T_d + T_e \end{aligned} \tag{4}$$

where U_s and U_b are the potential energy of the shaft and bearing, respectively. T_s and T_d are the kinetic energy of the shaft and disk, and T_e is the kinetic energy related to the eccentricity.

With the Lagrange approach

$$\frac{d}{dt}\left[\frac{\partial}{\partial \dot{q}_i}(T-U)\right]-\frac{\partial}{\partial q_i}(T-U)=0 \tag{5}$$

where $q_i=\{a_1,a_1,\cdots a_{N_p},b_1,b_1,\cdots b_{N_p}\}$

Substituting equation (4) into equation (5), the equation of motion can be expressed as:

$$\begin{bmatrix} M_T+M_R & 0 \\ 0 & M_T+M_R \end{bmatrix}\begin{Bmatrix}\ddot{a}\\ \ddot{b}\end{Bmatrix}+\Omega\begin{bmatrix} 0 & G \\ -G & 0\end{bmatrix}\begin{Bmatrix}\dot{a}\\ \dot{b}\end{Bmatrix} \tag{6}$$
$$+\begin{bmatrix} K_{yy} & K_{yz} \\ K_{zy} & K_{zz}\end{bmatrix}\begin{Bmatrix}a\\ b\end{Bmatrix}+\begin{bmatrix} K_S & 0 \\ 0 & K_S\end{bmatrix}\begin{Bmatrix}a\\ b\end{Bmatrix}=\begin{Bmatrix}R_a\\ R_b\end{Bmatrix}$$

where $a=\{a_1,a_2,\cdots a_{N_p}\}^T$, $b=\{b_1,b_2,\cdots b_{N_p}\}^T$, $[M_T],[M_R]$, $[G]$, $[K_S]$, $[K_{yy}]$, $[K_{yz}]$, $[K_{zy}]$ and $[K_{zz}]$ are $N_P\times N_P$ real symmetric matrices, which are expressed as:

$$M_T(m,n)=\int_0^l A\rho x^{m+n-2}dx+\sum_{i=1}^{N_d}m_i^d(x_i^d)^{m+n-2}$$
$$M_R(m,n)=(m-1)(n-1)\left\{\int_0^l I_D x^{m+n-4}dx+\sum_{i=1}^{N_d}I_{Di}^d(x_i^d)^{m+n-4}\right\}$$
$$G(m,n)=(m-1)(n-1)\left\{\int_0^l I_P x^{m+n-4}dx+\sum_{i=1}^{N_d}I_{Pi}^d(x_i^d)^{m+n-4}\right\} \tag{7}$$
$$K_S(m,n)=(m-1)(m-2)(n-1)(n-2)\int_0^l EIx^{m+n-6}dx$$
$$K_{yy}(m,n)=\sum_{j=1}^{N_b}k_{yyj}^b(x_j^b)^{m+n-2},\ K_{yz}(m,n)=\sum_{j=1}^{N_b}k_{yzj}^b(x_j^b)^{m+n-2}$$
$$K_{zy}(m,n)=\sum_{j=1}^{N_b}k_{zyj}^b(x_j^b)^{m+n-2},\ K_{zz}(m,n)=\sum_{j=1}^{N_b}k_{zzj}^b(x_j^b)^{m+n-2}$$

R_a and R_b are the form of

$$R_a=\{R_{a1},R_{a2},\cdots R_{aN_p}\}^T$$
$$R_b=\{R_{b1},R_{b2},\cdots R_{bN_p}\}^T \tag{8}$$

where

$$R_a=\int_0^l e(x)\rho(x)A(x)\Omega^2\cos(\Omega t+\varphi)x^{N_P-1}dx$$
$$+\sum_{i=1}^{N_d}m_i^d(e_i^d)\Omega^2\cos(\Omega t+\varphi_i^d)(x_i^d)^{N_P-1} \tag{9}$$
$$R_b=\int_0^l e(x)\rho(x)A(x)\Omega^2\sin(\Omega t+\phi)x^{N_P-1}dx$$
$$+\sum_{i=1}^{N_d}m_i^d(e_i^d)\Omega^2\sin(\Omega t+\varphi_i^d)(x_i^d)^{N_P-1}$$

Ⅲ. SIMILARITY TRANSFORMATION AND NORMALIZE

The other assumed mode functions, which are based on the GAMM, will be derived and applied in this paper. The governing equations can be assumed as Legendre polynomials and Chebyshev polynomials model by using the similarity transformation matrix.

3.1 Classical Orthogonal Polynomials

In mathematics, an orthogonal polynomial sequence is an infinite sequence of polynomials for one variable x. The sequence $P_n=[P_1,P_2,\cdots P_n]$ has n degrees and any different two polynomials in this sequence are orthogonal to each other by definition the inner product. The simplest classical orthogonal polynomials are the Legendre polynomials, which interval of orthogonality is [−1, 1], and the weight function is a simply one.

$$\int_{-1}^{1}P_m(x)P_n(x)dx=0 \tag{10}$$

Let $P_n(x)$ be the Legendre polynomial with n degrees, and choose $P_0=1$ and $P_1=x$. The recursion formula for the Legendre polynomial is

$$(n+1)P_{n+1}(x)=(2n+1)xP_n(x)-nP_{n-1}(x) \tag{11}$$

With equation (11) the sequence Legendre polynomial can be generated easily. The first six polynomials of the sequence are shown in Figure 2.

The Chebyshev polynomials are orthogonal with the inner product

$$\int_{-1}^{1}T_m(x)T_n(x)(1-x^2)^{-1/2}dx=0 \tag{12}$$

where

$$T_0(x)=1,\quad T_1(x)=x,\quad T_{n+1}(x)=2xT_n(x)-T_{n-1}(x) \tag{13}$$

The first six Chebyshev polynomials are shown in Figure 3

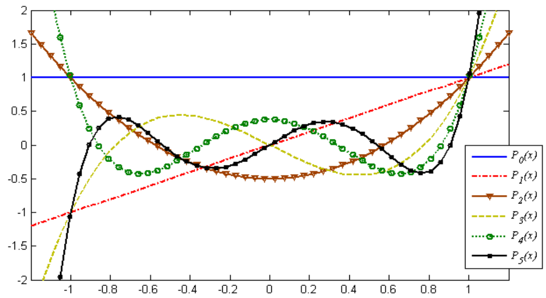

Figure 2 The first six sequence of Legendre polynomial.

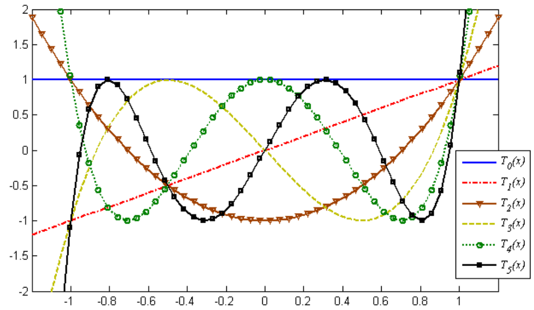

Figure 3 The first six sequence of Chebyshev polynomial.

Both the Legendre and Chebyshev polynomials are based on generalized polynomial $[1, x, x^2, \cdots, x^{N_P-1}]$, therefore equation (11) and (13) can be arranged as the matrix form:

$$\begin{Bmatrix} P_0(x) \\ P_1(x) \\ P_2(x) \\ P_3(x) \\ P_4(x) \end{Bmatrix} = [P]_{N_P \times N_P} \begin{Bmatrix} 1 \\ x \\ \cdots \\ x^{N_P-1} \end{Bmatrix}_{N_P \times 1} \tag{14}$$

and

$$\begin{Bmatrix} T_0(x) \\ T_1(x) \\ T_2(x) \\ T_3(x) \\ T_4(x) \end{Bmatrix} = [T]_{N_P \times N_P} \begin{Bmatrix} 1 \\ x \\ \cdots \\ x^{N_P-1} \end{Bmatrix}_{N_P \times 1} \tag{15}$$

The matrices $[P]$ and $[T]$ represent the similarity transformation matrix, $[P]$ is the Legendre polynomial similarity transformation, and [T] is the Chebyshev polynomial similarity transformation. In this paper, $[P]$ and $[T]$ are signed as [S]. With the similarity transformation matrix [S], equation (3) can be rewired as

$$V(x,t) = \begin{Bmatrix} a_1 & a_2 & \cdots & a_{N_P} \end{Bmatrix}_{1 \times N_P} [S]_{N_P \times N_P} \begin{Bmatrix} 1 \\ x \\ \vdots \\ x^{N_P-1} \end{Bmatrix}_{N_P \times 1}$$

$$W(x,t) = \begin{Bmatrix} b_1 & b_2 & \cdots & b_{N_P} \end{Bmatrix}_{1 \times N_P} [S]_{N_P \times N_P} \begin{Bmatrix} 1 \\ x \\ \vdots \\ x^{N_P-1} \end{Bmatrix}^T_{N_P \times 1} \tag{16}$$

Substituting equation (16) into equations (6), the system equation of motion with orthogonal polynomial can be represented as

$$[L]^T \begin{bmatrix} M_T + M_R & 0 \\ 0 & M_T + M_R \end{bmatrix} [L] \begin{Bmatrix} \ddot{a} \\ \ddot{b} \end{Bmatrix} + \Omega [L]^T \begin{bmatrix} 0 & G \\ -G & 0 \end{bmatrix} [L] \begin{Bmatrix} \dot{a} \\ \dot{b} \end{Bmatrix}$$
$$+ [L]^T \begin{bmatrix} K_{yy} & K_{yz} \\ K_{zy} & K_{zz} \end{bmatrix} [L] \begin{Bmatrix} a \\ b \end{Bmatrix} + [L]^T \begin{bmatrix} K_S & 0 \\ 0 & K_S \end{bmatrix} [L] \begin{Bmatrix} a \\ b \end{Bmatrix} = [L]^T \begin{Bmatrix} R_a \\ R_b \end{Bmatrix} \tag{17}$$

were $$[L] = \begin{bmatrix} [S] & 0 \\ 0 & [S] \end{bmatrix} \tag{18}$$

3.2 Normalize of Shaft Length

In the process of applying GAMM, the numerical instability will occur in the higher order terms when the shaft length is not equal the distance of end points in [-1,1]. In the applying of the assumed mode method, normalize of length means using a different assumed mode function. The orthogonality intervals of both the Legendre and Chebyshev polynomial are [−1, 1]. The optimal interval of generalized polynomials interval is the same as [−1, 1], for the reason that the interval of assumed mode function is consistent with the shaft length. Therefore, using shifting function to convert the interval can prevent numerical instability and improve convergence. For example, the shifting function is defined as $\tilde{\phi}(x) = \phi(2x-1)$. As the shifting function is changed, the interval is converted from [0,1] to [-1, 1]. Figures (4) and (5) show the first six sequences of generalized polynomial $\phi(x)$ and $\tilde{\phi}(x)$ individually.

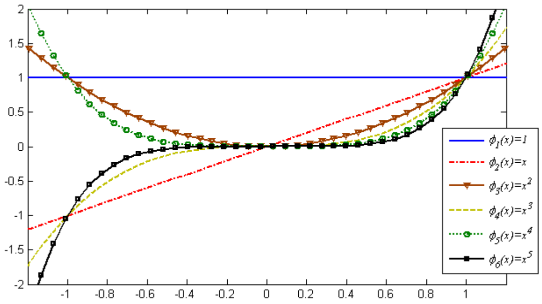

Figure 4 The first six sequence of generalized polynomial $\phi(x)$

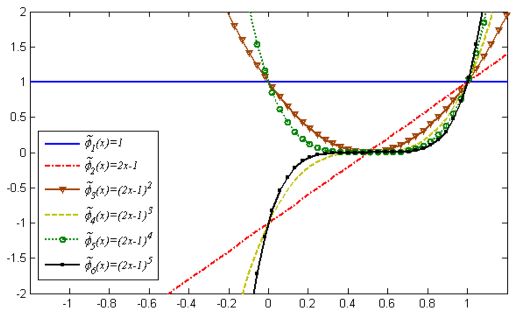

Figure 5 The first six sequence of generalized polynomial $\tilde{\phi}(x)$

IV. NUMERICAL RESULTS AND DISCUSSIONS

Three cases are discussed in this paper. Case 1 studies the multi-stepped rotor system, which are used to illustrate the accuracy of the GAMM, FEM, and GAMM based on Legendre and Chebyshev polynomials. Case 2 studies the dual rotor-bearing system, and discusses the convergence of the critical speed with GAMM at different intervals. Case 3 studies the multi-shaft rotor-bearing system, and also discusses the effects of bearing stiffness and contact stiffness on the critical speeds.

Case 1:

The Nelson's rotor system model [2] is applied to illustrate the accuracy of GAMM, FEM and the GAMMs based on Legendre and Chebyshev polynomials. Figure 6 and Table 1 show the configuration of the rotor system and corresponding data. Table 2 shows the whirl speeds with Legendre, Chebyshev, GAMM and FEM. The whirl speed map is shown in Figure 7. In Figure 7, the polynomial numbers N_P for GAMM, Legendre and Chebyshev are selected as 23, and the element number for FEM is selected as 18. As this figure shown, the GAMM, Legendre and Chebyshev have the same result in whirl speed map, but the result is different with the FEM. Figure 8 shows the first three eigen-modes with forward and backward motions, which indicates that by using the GAMM, Legendre, Chebyshev and FEM can get similar results in the first two modes. In the third mode, the results are different slightly. The percentages of difference for whirl speeds of the first five terms are lower than 5.0%.

Table 1 Multi-stepped rotor configuration data of Case 1

Density=7806 Kg/m^3		Elastic modulus=2.078×10^{11} N/m^2			
Disk：	Location (cm)	Mass (Kg)		Polar inertia (Kg.m^2)	Diametral inertia (Kg.m^2)
D1	-9.01	1401		0.002	0.00136
Bearing：	Location (cm)	K_{yy}=K_{zz} (10^7 N/m)		K_{yz}=K_{zy} (10^7 N/m)	
B1	-1.39	3.503		-0.8756	
B2	10.8	3.503		-0.8756	
Node no.	Node location (cm)	Element length (cm)	Bearing & Disk	Outer radius (cm)	Inner radius (cm)
1	-17.9	1.27		0.51	0
2	-16.63	3.81		1.02	0
3	-12.82	2.54		0.76	0
4	-10.28	1.27		2.03	0
5	-9.01	1.27	D 1	2.03	0
6	-7.74	0.51		3.3	0
7	-7.23	0.76		3.3	1.52
8	-6.47	1.27		2.54	1.78
9	-5.2	0.76		2.54	0
10	-4.44	3.05		1.27	0
11	-1.39	2.54	B 1	1.27	0
12	1.15	3.81		1.52	0
13	4.96	3.81		1.52	0
14	8.77	2.03		1.27	0
15	10.8	1.78	B 2	1.27	0
16	12.58	1.02		3.81	0
17	13.6	3.04		2.03	0
18	16.64	1.27		2.03	1.52
19	17.91	-		-	-

Table 2 The whirl speeds using Legendre, Chebyshev, GAMM and FEM of Case 2

Rotating Speed (Ω, rad/sec)	whirl speed (ω_r, rad/sec)							
	Legendre (N_P=23)		Chebyshev (N_P=23)		GAMM (N_P=23)		FEM (Ne=18)	
	F	B	F	B	F	B	F	B
2000.0	1760.2	1466.4	1759.8	1466.7	1760.0	1466.5	1719.8	1459.8
	5063.9	4177.5	5064.0	4176.9	5064.1	4177.4	4997.6	4140.9
	8502.9	7127.2	8503.0	7127.5	8502.7	7127.1	8019.4	6925.3
3000.0	1788.8	1438.3	1788.8	1438.3	1788.7	1438.3	1737.2	1441.6
	5062.4	4174.1	5062.4	4174.0	5062.5	4174.1	4999.6	4136.3
	8680.4	6994.9	8680.4	6994.9	8680.3	6994.8	8061.2	6875.7
4000.0	1822.2	1405.8	1821.5	1405.6	1822.1	1405.7	1758.2	1419.4
	5060.2	4169.1	5059.9	4171.8	5060.1	4169.5	5002.2	4130.0
	8888.2	6850.0	8887.3	6849.6	8888.2	6849.9	8113.0	6813.1
5000.0	1858.1	1370.7	1858.9	1371.1	1858.0	1370.7	1781.5	1394.7
	5056.6	4163.6	5058.8	4158.2	5056.9	4163.5	5005.5	4122.0
	9115.2	6703.0	9115.9	6703.6	9115.1	6702.9	8170.8	6741.5
6000.0	1895.4	1334.7	1895.5	1334.8	1895.2	1334.7	1806.1	1368.5
	5052.5	4155.8	5053.1	4154.6	5052.6	4156.1	5009.3	4112.4
	9355.1	6559.4	9355.2	6559.6	9355.0	6559.3	8231.3	6664.1

† The interval of Legendre, Chebyshev and GAMM is [−0.18, 0.18] meter
‡ Np：number of polynomial; Ne：number of element
F：forward; B：backward

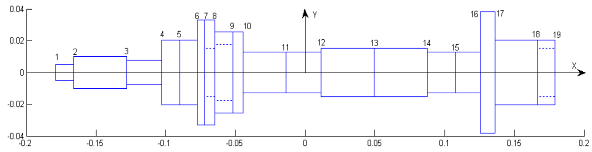

Figures 6 The rotor configuration of Case 1

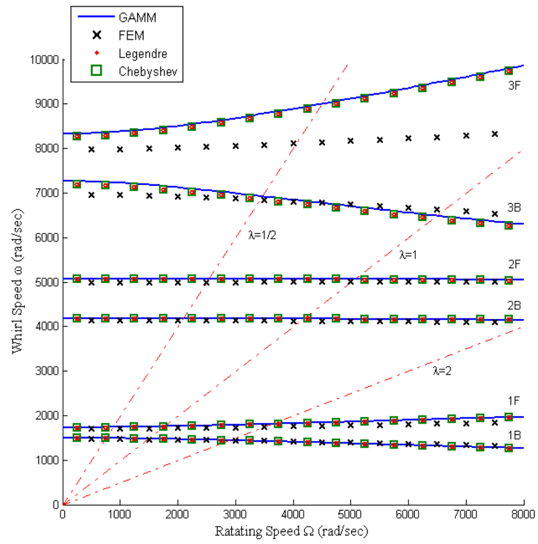

Figures 7 The whirl speed map of Case 1.

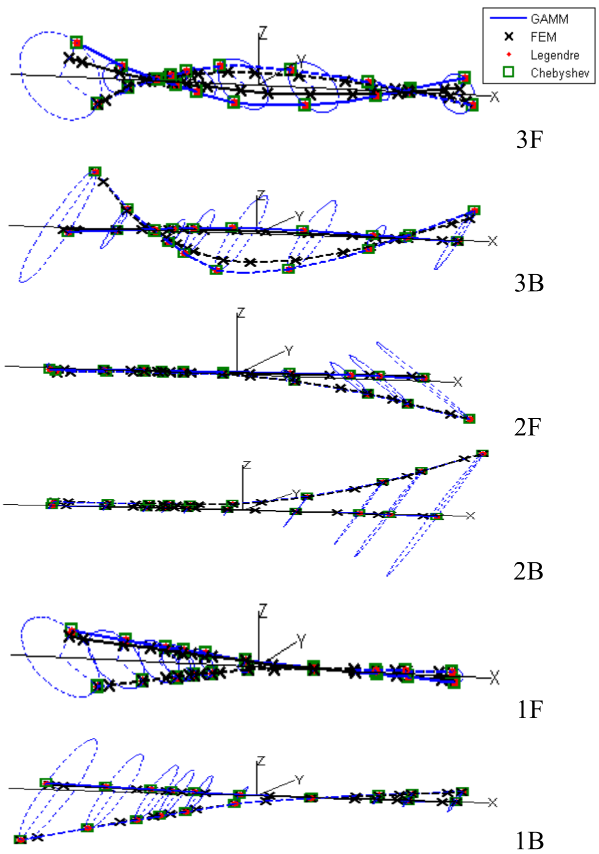

Figures 8 First three eigenmodes of Case 1 for Ω=2000 rad/sec.

Case 2:

The rotor system with multiple shafts is studied by Rajan [9] and Shiau [10]. Figure 9 and Table 3 show the configuration and parameters of this dual rotor system. The inner shaft denotes shaft 1 with rotating speed Ω_1 and the outer shaft denotes shaft 2 with rotating speed $\Omega_2=1.5\Omega_1$. Figure 10 shows the whirl speed map and Table 4 shows the synchronous line $\lambda=1$ and $\lambda=2/3$ of the critical speeds by the FEM and GAMM. The percentages of difference between the first six terms are lower than 2.0%. Table 5 shows the convergence analysis of the critical speed at different intervals. The two shafts can be assumed with different mode function individually. Therefore, two polynomial functions of different intervals are used in the dual rotor system. In addition, as shown in Table 5, adjusting the interval of polynomial functions and improving polynomial numbers can increase the accuracy. Figure 11 shows the comparison of forward mode shapes with the GAMM and FEM.

Table 3 The dual rotor configuration data of Case 2.

	Node no.	Node location (cm)	Element length (cm)	Bearing & Disk	Outer radius (cm)	Inner radius (cm)
shaft 1	1	0	7.62	B 1	1.524	0
	2	7.62	17.78	D 1	1.524	0
	3	25.4	15.24		1.524	0
	4	40.64	5.08	B c	1.524	0
	5	45.72	5.08	D 2	1.524	0
	6	50.8	-	B 2	-	-
shaft 2	7	15.24	5.08	B 3	2.542	1.905
	8	20.32	15.24	D 3	2.542	1.905
	9	35.56	5.08	D 4	2.542	1.905
	10	40.64	-	B c	-	-

Density=8304 Kg/m^3 Elastic modulus=2.069×10^{11} N/m^2

Disk：	Location (cm)	Mass(Kg)	Polar inertia ($Kg.m^2$)	Diametral inertia ($Kg.m^2$)
D1	7.62	4.904	0.0271	0.0135
D2	45.72	4.203	0.0203	0.0101
D3	20.32	3.327	0.0146	0.0073
D4	35.56	2.277	0.0097	0.0048

Bearing：	Node	$K_{yy}=K_{zz}$(10^6 N/m)	$K_{yz}=K_{zy}$
B1	1	26.2795	0
B2	6	17.5197	0
B3	7	17.5197	0
Bc	4 - 10	8.7598	0

Table 4 The critical speeds of Case 2.

GAMM (Np=27)				FEM (Ne=16)			
$\omega=\Omega_1$(rad/sec)		$\omega=\Omega_2$(rad/sec)		$\omega=\Omega_1$(rad/sec)		$\omega=\Omega_2$(rad/sec)	
$\lambda=1$	$\lambda=-1$	$\lambda=2/3$	$\lambda=-2/3$	$\lambda=1$	$\lambda=-1$	$\lambda=2/3$	$\lambda=-2/3$
Forward	Backward	Forward	Backward	Forward	Backward	Forward	Backward
867.74	660.38	824.95	687.17	853.72	664.00	815.83	689.40
1615.05	1439.16	1593.38	1475.47	1595.13	1443.46	1575.52	1473.80
2306.58	2141.21	2295.78	2190.63	2277.51	2157.16	2268.06	2194.42
4389.70	2319.18	3678.92	2517.63	3625.49	2289.58	3314.87	2478.53
5595.16	2470.52	4934.04	2560.14	5411.93	2474.66	4833.47	2603.81

† The interval of GAMM is [−0.3, 0.3] meter

‡ Np：number of polynomial; Ne：number of element

Table 5 Convergence analysis of the critical speed at different intervals for Case 2

		Np=8	Np=10	Np=12	Np=14	Np=15	Np=16	Np=18
shaft 1	1F	868.18	868.04	867.94	867.91	867.91		
shaft 2	2F	1617.33	1616.10	1615.68	1615.44	1615.40		
[±1]	3F	2313.77	2309.19	2308.16	2307.12	2306.96		
	4F	4426.28	4419.97	4404.50	4402.18	4401.56		
	5F	5872.11	5778.01	5681.29	5666.70	5651.32		
	6F	21252.30	17620.51	17544.67	17184.01	17156.24		
		Np=24	Np=26	Np=27	Np=28	Np=29	Np=30	Np=31
shaft 1	1F	867.75	867.74	867.74	867.74	867.74		
shaft 2	2F	1615.09	1615.06	1615.05	1615.06	1615.04	1615.02	1615.02
[±0.3]	3F	2306.58	2306.57	2306.58	2306.57	2306.57	2306.01	
	4F	4389.68	4388.33					
	5F	5602.23	5596.70	5595.16	5593.75	5593.50		
	6F	16826.35	16757.42	16743.50				
		Np=18	Np=24	Np=26	Np=27	Np=28	Np=29	Np=30
shaft 1	1F	867.82	867.75	867.74	867.74	867.74	867.74	867.74
[±0.3]	2F	1615.24	1615.09	1615.06	1615.05	1615.06	1615.04	
shaft 2	3F	2306.68	2306.58	2306.58	2306.57	2306.57	2306.57	2306.57
[±,0.2]	4F	4393.46	4389.83	4389.60	4386.93			
	5F	5624.90	5602.24	5596.71	5595.11	5593.74	5593.57	
	6F	16962.66	16826.35	16757.41	16743.51			

：numerical unstable

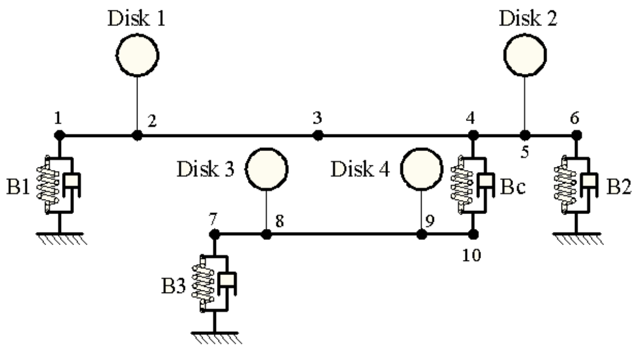

Figures 9 The dual rotor model of Case 2.

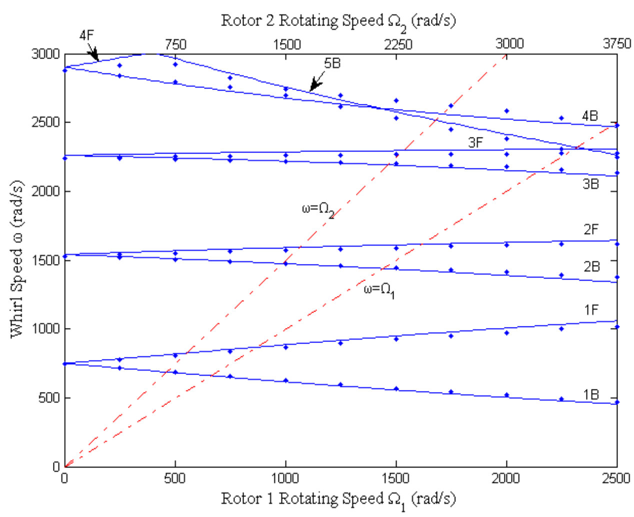

Figures 10 The whirl speed map of Case 2.

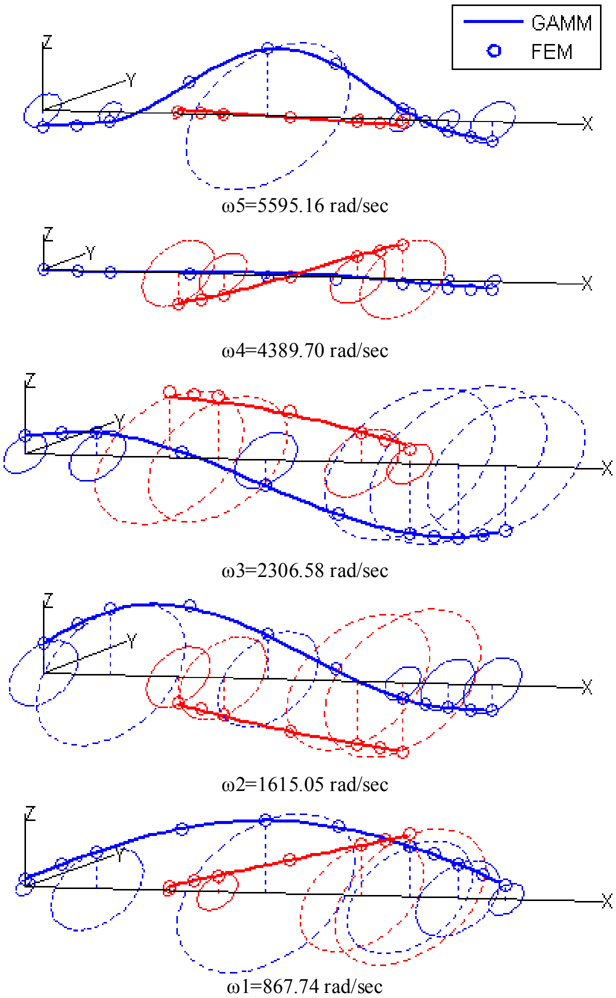

Figures 11 Mode shapes of Case 2 for λ=1

Case 3:

The multi-shaft rotor configuration is shown in Figure 12, which consists of two isotropic bearings, two rigid disks and three shafts for single speed. The multi-shaft rotor system is composed of different types of combinations and the system model is assumed to be the three-shaft system as Figure 13. The configuration data are given in Table 6. The numerical results of critical speeds using GAMM and FEM are shown in Table 7, and mode shapes using GAMM and FEM are shown in Figure 14. The percentages of difference are lower than 5.6%. Similarly, Figure 15 shows the corresponding whirl speed and Figure 16 shows the critical speeds with bearing stiffness in the region 10^5 to 10^9 (N/m). Figure 17 shows the critical speeds with the change in contact stiffness. According to the results, the bearing stiffness has great influence in critical speed.

Table 6 The multi-shaft rotor configuration data of Case 3.

Shaft No.	Densityρ(Kg/m^3)	Elasticity E(N/m^2)	poisson ratio γ
shaft 1	7800	1.960×10^{11}	0.28
shaft 2	8010	1.957×10^{11}	0.35
shaft 3	7900	2.00×10^{11}	0.29
Disk：	Mass (kg)	Diametral inertia (Kg.m^2)	Polar inertia (Kg.m^2)
D1	5.5	0.0202	0.04
D2	1.8	0.0059	0.0115
Bearing：	K_{yy}=K_{zz}	K_{yz}=K_{zy}	
B1	1×10^7 (N/m)	0	
B2	1×10^7 (N/m)	0	
Contact stiffness：			
Kc1	1×10^9 (N/m)	0	
Kc2	1×10^9 (N/m)	0	
Kc3	1×10^9 (N/m)	0	
Kr2	1×10^9 (N · m/rad)	0	
Kr3	1×10^9 (N · m/rad)	0	

Table 7 The convergence analysis of critical speeds using GAMM and FEM for Case 3.

	Np=17	Np=18	Np=19	Ne =45	GAMM (Np=19)	FEM (Ne =45)	difference(%)
1F	795.85	795.85	795.84	792.28	795.84	792.28	0.45
2F	1027.50	1027.45	1027.44	1009.45	1027.44	1009.45	1.75
3F	1857.36	1857.31	1857.33	1818.11	1857.33	1818.11	2.11
4F	2567.94	2567.81	2567.58	2540.36	2567.58	2540.36	1.06
5F	5308.01	5308.03	5307.70	5171.98	5307.70	5171.98	2.56
6F	6050.44	6050.34	6051.16	5712.32	6051.16	5712.32	5.60

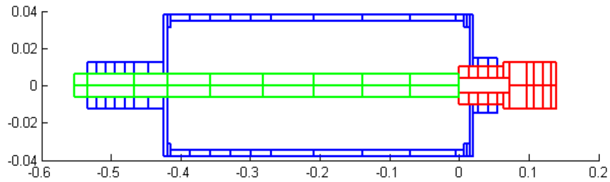

Figures 12 The multi-shaft rotor configuration of Case 3.

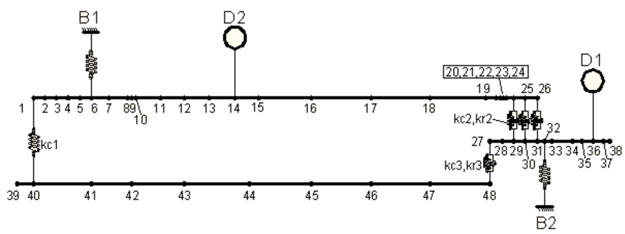

Figures 13 The three shaft model of Case 3.

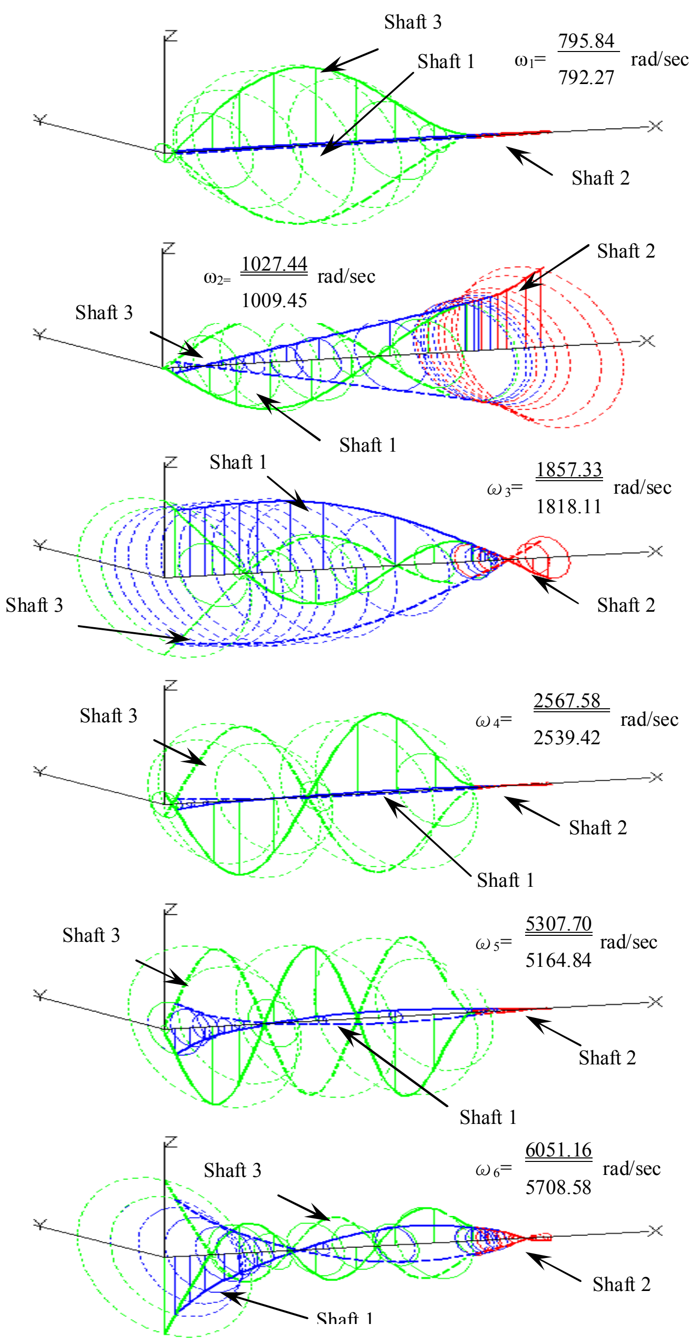

Figures 14 The comparison of mode shapes and potential energy for Case 3. (continue)

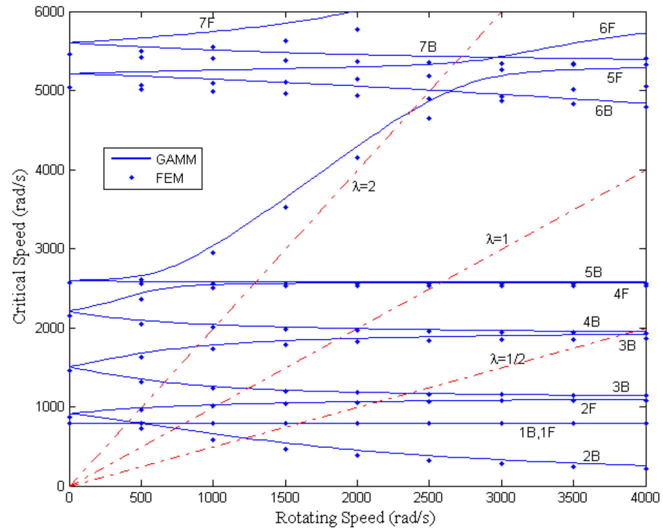

Figures 15 The whirl speed map of Case 3.

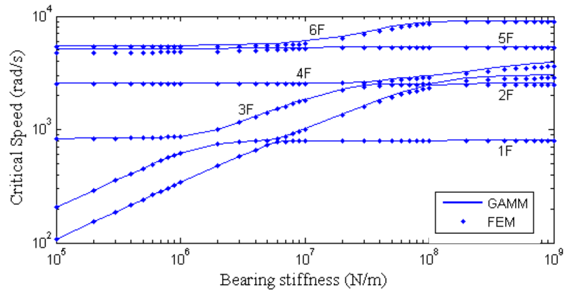

Figures 16 Effects of bearing stiffness B1 and B2 on the critical speeds for Case 3.

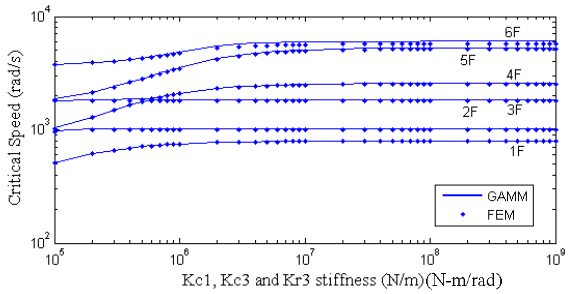

Figures 17 Effects of the contact stiffness of shaft-3 on the critical speeds for Case 3

V. CONCLUSIONS

This paper investigates the dynamic analysis of a rotor bearing system with linear supports using the Global Assumed Mode Method (GAMM) for different polynomials. The Finite Element Method (FEM) is also applied to compare the results with this assumed mode method. As the results show, both the GAMMs based on Legendre and Chebyshev polynomials are feasible to analyze the dynamic characteristics of rotor bearing systems. The polynomial number can be increased as the interval of the assumed mode function is altered, and the convergence of high order mode will be accurate more.

VI. REFERENCES

[1] Ruhl, R.L. and Booker, J.F., 1972, "A finite element model for distributed parameter turbo rotor systems". *ASME journal of Engineering for industry*, **94**, pp.126-132.

[2] Nelson, H.D. and McVaugh, J.M., 1976, "The dynamics of rotor-bearing systems using finite element''. *ASME journal of Engineering for industry*, **98**, pp.593-600.

[3] Zorzi, E.S. and Nelson, H.D., 1977, "Finite element simulation of rotor bearing system with internal damping''. *ASME journal of Engineering for Power*, pp.71-76.

[4] Nelson,H.D., 1980, "A finite rotating shaft element using Timoshenko beam theory''. *ASME journal of Mechanical Design*, **102**, pp.793-803.

[5] Özgüvent, H. Nevzat, Z. and Levent, Özkan, 1984, "Whirl speeds and unbalance response of multibearing rotors Using Finite Elements". *Journal of Vibration, Acoustics, Stress, and Reliability in design*, **106**, pp.72-79.

[6] Greenhill, L.M., Bickford, W.B. and Nelson, H.D., 1985, "A conical beam finite element for rotor dynamics analysis''. *ASME journal of Vibration,Acoustic,Stress,and Reliability in design*, **107**, pp.421-430.

[7] Tsuchiya, K., 1982, "Passage of a rotor through a critical speed''. Transaction of the *ASME journal of Mechanical Design*, **104**, pp.370-374.

[8] Lund, J.W., 1979, "Sensitivity of the critical speed of a rotor to change in the design''. *ASME journal of Mechanical Design*, **102**, pp.115-121.

[9] Rajan, M., Nelson, H.D.,and Chen, W.J., 1986, "Parameter sensitivity in the dynamics of rator-bearing system''. Transaction of the *ASME journal of Vibration, Acoustic, Stress, and Reliability in design*, **108**, pp.197-206.

[10] Shiau, T.N. and Hwang, J.L., 1989, "A new approach to the dynamic characteristic of undamped rotor-bearing systems''. *ASME journal of Vibration, Acoustic, Stress, and Reliability in design*, **111**, pp.379-385.

[11] Hwang, J.L and Shiau, T.N., 1991, "An application of generalized polynomial expansion method to nonlinear rotor bearing systems". *ASME Journal of Vibration and Acoustics*, **113**, pp.299-308.

[12] Shiau, T.N. and Hwang, J.L., 1993, "Generalized polynomial expansion method for the dynamic analysis of rotor-bearing systems". *ASME Journal of Engineering for Gas Turbine and Power*, **115**, pp.209-217.

[13] Shiau, T.N., Chen, E.C., Huang, K.H. and Hsu, W.C., 2006, "Dynamic response of a spinning Timoshenko beam with general boundary conditions under a moving skew force using global assumed mode method". *JSME International Journal of the Japan Society of Mechanical Engineers*, **49**, pp.401-410.